**The comparision of glybenclamide and metformin-loaded bacterial cellulose/gelatin nanofibres produced by a portable electrohydrodynamic gun for diabetic wound healing**

**Muhammet Emin Cam**[a,b,c,*], Maryam Crabbe-Mann[a], Hussain Alenezi[a,d], Ayse Nur Hazar-Yavuz[c], Busra Ertas[c], Ceyda Ekentok[e], Gul Sinemcan Ozcan[f], Fadime Topal[c], Ece Guler[b,c], Yusufhan Yazir[f], Maryam Parhizkar[g], Mohan Edirisinghe[a,*]

*Corresponding authors

[a]Department of Mechanical Engineering, University College London, Torrington Place, London WC1E 7JE, UK

[b]Center for Nanotechnology and Biomaterials Research, Marmara University, Istanbul 34722, Turkey

[c]Department of Pharmacology, Faculty of Pharmacy, Marmara University, Istanbul 34668, Turkey

[d]Department of Manufacturing Engineering, College of Technological Studies, PAAET, 13092 Kuwait City, Kuwait

[e]Department of Pharmaceutical Biotechnology, Faculty of Pharmacy, Marmara University, Istanbul 34722, Turkey

[f]Stem Cell and Gene Therapies Research and Applied Center, Medical Faculty, Kocaeli University, Kocaeli 41380, Turkey

[g]School of Pharmacy, University College London, London, WC1N 1AX, UK

*Corresponding Authors (Muhammet Emin Cam, Mohan Edirisinghe); Postal address: Department of Mechanical Engineering, University College London, Torrington Place, Roberts Building, London WC1E 7JE, UK; Tel: +44 (0)75 0606 1425; Fax: +44 (0)20 7388 0180; e-mail addresses: m.cam@ucl.ac.uk, m.edirisinghe@ucl.ac.uk

Maryam Crabbe-Mann, Hussain Alenezi

Postal address: Department of Mechanical Engineering, University College London, Torrington Place, Roberts Building, London WC1E 7JE, UK; Tel: +44 (0)75 0606 1425; Fax: +44 (0)20 7388 0180; e-mail addresses: maryam.crabbe-mann.14@ucl.ac.uk, hussain.alenezi.18@ucl.ac.uk

Ayse Nur Hazar-Yavuz, Busra Ertas, Fadime Topal, Ece Guler, Ceyda Ekentok

Postal address: Marmara University Faculty of Pharmacy Tıbbiye Street No: 49, Haydarpasa 34668 Istanbul / Turkey; Tel: +90 216 414 29 62; Fax: +90 216 345 29 52; e-mail addresses: ayse.hazar@marmara.edu.tr, busra.ertas@marmara.edu.tr, fatmafadimetopal@gmail.com, eczeceguler@gmail.com, ceyda.ekentok@marmara.edu.tr

Gul Sinemcan Ozcan, Yusufhan Yazir

Postal address: Kocaeli Universitesi Umuttepe Yerleskesi Morfoloji Binasi Kat:1 41380 Umuttepe/Kocaeli; Tel: +90 0262 303 86 85; Fax: +90 0262 359 12 78; e-mail address: gulsinemcan@hotmail.com, yusufhan.yazir@kocaeli.edu.tr

Maryam Parhizkar

Postal address: School of Pharmacy, University College London, London, WC1N 1AX, UK; Tel: +44 (0)20 7753 5800; Fax: +44 (0)20 7753 5829; e-mail addresses: maryam.parhizkar@ucl.ac.uk

## ABSTRACT

Wound dressings made from natural polymers are an important aspect of biomaterials. Protein-based materials are less likely to instigate an immunogenic response and have the capacity to degrade *in vivo*, also without triggering an inflammatory response. Therefore, gelatin (GEL) was chosen and combined with bacterial cellulose (BC) to produce nanofibres and the potential of an all-natural polymer construct was determined. GEL and BC were successfully electrospun with metformin (Met) and glybenclamide (Gb) using a portable, point of need electrospinning set up. The virgin fibre group exhibited a significant effect on the proliferation of L929 (mouse fibroblast) cells but all fibre samples can safely be applied on wound site without risk of cytotoxicity. According to the results obtained by animal tests, the GEL-BC-Gb group showed better recovery than the GEL-BC-Met group. Diabetic wounds treated with GEL-BC-Met were characterized by moderate re-epithelialization and partially organized granulation tissue. Moderate to complete re-epithelialization and well-formed granulation tissue were observed in diabetic wounds treated with GEL-BC-Gb. The histologic scores obtained on day 14 confirmed

that the GEL-BC-Gb group played a stronger wound-healing role compared to the GEL-BC-Met group. The highest decrease of TNF-α level was observed in the GEL-BC-Gb group at the end of the experiment but there is no significant difference between drug-loaded fibre groups. Therefore, topical administration of Met and Gb in a sustained release form has a high potential for diabetic wound healing with high bioavailability and fewer systemic side effects but Gb showed better improvement according to the results of the animal tests.

**KEYWORDS:** *Bacterial cellulose, Gelatin, Wound dressings, Oral antidiabetic agents, Drug release, Portable electrohydrodynamic gun*

## 1. Introduction

Diabetes mellitus (DM) is a group of metabolic disorders characterized by hyperglycemia following insulin resistance and/or deficiency in insulin secretion [1, 2]. One of the most common serious complications of diabetes is peripheral neuropathy with risk of foot ulcers and amputations [3].

It has been suggested that the diabetic environment i.e. hyperglycemia, promotes a pro-inflammatory phenotype of macrophages. These macrophages, purposed with killing pathogens and removing damaged tissue, release pro-inflammatory cytokines such as tumour necrosis factor-α (TNF- α), interleukin-1 beta (IL-1β) and interleukin-6 (IL-6) at a sustained level, preventing the progression of the healing process and the consequent release of anti-inflammatory cytokines and growth factors [4-6]. There has also been research investigating the persistent presence of cytokine precursors; such as Nod-like receptor protein (NLRP3) and caspase-1, in diabetic wounds disrupting the healing process [7].

Glybenclamide (Gb), is a common oral treatment for type II diabetes, from a class of drugs known as sulfonylureas. Mirza et al. demonstrated the application of Gb in pluronic gel to wounds excised on *db/db* mice accelerated re-epithelialisation and granulation tissue. Also, Gb reduced the level of inflammatory cytokines whilst increasing the pro-healing cytokines [7]. Whilst comparing the effectiveness of glybenclamide to glimepiride (another sulfonylurea) within a group of diabetic patients (delivered orally), glybenclamide brought about a reduction in the levels of various inflammatory cytokines [8]. Gb has been shown to specifically inhibit the action of NRLP-3, due to the presence of the sulfonyl and benzamido groups on the Gb molecule, these disrupt the biomolecular cascade that brings about NRLP-3 secretion [9]. Metformin (Met) is typically the first port of call in the treatment of type II diabetes; it belongs

to a class of drugs known as biguanides. The effect of Met on inflammation has yet to be demonstrated on humans, but its effect on murine macrophages has been described in the literature. Nath et al. showed the application of Met to RAW267.4 cells reduced a number of pro inflammatory cytokines; IFN-γ, TNF-α, IL-6, IL-7 and inducible NO synthase [10]. A more relevant example of Met used in wound healing was shown by Lee et al. [11]. Poly-lactic-glycolic (PLGA) and Met were electrospun and applied to diabetic induced rat wounds. The PLGA-Met fibres brought about greater wound closure after 14 days (2.9 ± 0.8% ), compared to wounds treated with virgin PLGA (15.5 ± 1.4%) and the control treated with a conventional gauze (2.9 ± 0.8% ) [11]. Met has also been used to successfully reduce tumour necrosis factor and tissue factor [12].

Microfibrils of bacterial cellulose (BC) were about 100 times thinner than plant cellulose. BC fibers have higher specific area, higher water holding capacity, and longer drying time compared to plant-cellulose. Moreover, the molecular structure of BC is the same as that of plant cellulose, except for its polymerization degree, which is 13000 to 14000 for plants and 2000 to 6000 for BC [13]. Its biocompatibility and resemblance to the extra cellular matrix has led to its introduction to the medical sector where it has been successfully used as artificial skin in treating burns, and artificial blood vessels in microsurgery [14-16]. BC is easily sterilised and has been found to be non-allergenic, these characteristics as well as the many others have made it a major candidate for use as wound dressing [17]. Gelatin (GEL) is another popular choice in biomaterials, especially as cellular scaffolds, as the extracellular matrix is mostly made up of proteins [18, 19]. GEL is a protein derived from partial hydrolysis of collagen. GEL has some advantages compared to collagen such as high biocompatibility and biodegradability and does not cause immune rejection problems due to its high water-holding capacity. Nanofibres with GEL absorb the wound exudate, maintain nutrient transport and molecular signals that may control cell behaviour. Thus, cell growth and proliferation are improved and as a result wound healing is accelerated [20]. In a composite of BC and GEL, BC will perform as a scaffold, and GEL in its network creates an ideal wound dressing. The major conjugate force between GEL and BC is hydrogen bonds. This composite can be reinforced by crosslinking the two components [21]. Therefore, the composite was crosslinked with glutaraldehyde (GTA) vapour in our study.

GTA is the most widely preferred chemical to start the crosslinking reaction between BC and GEL due to its high efficiency [21]. The hypothesis is that GTA can crosslink BC and GEL and hence produce GEL/BC composites that can demonstrate significantly higher durability in

wet form, retain the original nanofibre morphology after immersion in water, and improve the thermal and mechanical properties when compared to simple blends of these polymers. This is a crucial feature for a nanofibre composite used in the treatment of wound healing. Nanofibres should have proper tensile strength so that it cannot be easily dispersed and therefore create a suitable area for the proliferation of fibroblast cells. This kind of crosslinked composites can be used as a substitute for tissues [22, 23].

In this paper, we report for the first time the production of an "all natural" drug eluting wound dressing using a portable, point of need electrospinning set up [24, 25]. BC was electrospun with gelatin to produce an "all natural" fibrous wound dressing. The fibres were doped with glybenclamide (Gel-BC-Gb) and metformin (Gel-BC-Met) and were crosslinked with glutaraldehyde vapour. These were produced using a portable, point of need electrospinning set up, and their effectiveness in healing diabetic ulcers in diabetic mice models were compared, with drug free gelatin-BC fibres. They were also assessed *in vitro* for their drug release profiles and their elemental constituents were examined.

The portable, point of need electrospinning set up has been used to successfully produce regenerative wound dressing that exhibited good biocompatibility and proliferation rates with Saos-2 cells [26]. Previously, Sofokleous et al. produced amoxicillin loaded PLGA fibres [27]. This set up has the potential to deposit wound dressing *in situ*, with the material conforming to the wound, even covering irregular shapes [25].

In the present study, the biological impact of Met and Gb-loaded fibres were examined in a 15-day wound-healing test in type-1 diabetic rats. Also wound tissues were histologically and biochemically investigated. Moreover, morphological evaluation, physical and chemical composition, thermal properties, drug release behaviors, and in-vitro cytotoxicity evaluation of all fibres were investigated.

## 2. Materials and methods

### *2.1. Materials*

Gelatin derived from bovine skin (40,000-50,000 g $mol^{-1}$), acetic acid ($CH_3COOH$), dimethylformamide (DMF) ($C_3H_7NO$), glybenclamide ($C_{23}H_{28}ClN_3O_5S$, molecular weight 494 g $mol^{-1}$), phosphate buffered saline tablets and glutaraldehyde ($C_5H_8O_2$) 50% in $H_2O$ were purchased Sigma-Aldrich (Poole, UK). Metformin-HCl ($C_4H_{12}ClN_5$, molecular weight: 129 g

mol-1**)** was purchased from APExBIO, Houston, USA. BC was provided by the Department of Medical Microbiology, Medipol University (Istanbul, Turkey).

*2.2. Preparation of solution*

Gelatin (Gel) solution was produced at 18wt% with acetic acid:water (80:20 weight ratio). The solution was prepared with magnetic stirrers overnight at room temperature. Bacterial cellulose (BC) mixture was made at 10wt% in dimethylformamide (DMF) only. The BC was homogenised (Branson Ultrasonic Sonifier S-250A, Fisher Scientific, UK) with DMF for 10 minutes. The Gel and BC were mixed at a ratio of 95:5 to which Met and Gb were added to form separate suspensions, at 4wt% and 1wt%, respectively.

*2.3. Portable electrohydrodynamic gun set up*

The portable EHD gun, shown in Fig. 1, is functionally identical to the table-top set up. A single needle (ID: 0.69 mm, OD: 1.07 mm, Stainless tube & Needle Co. Ltd, Staffordshire, UK) was encased in a repurposed spray gun. The needle was connected to 10 mL syringes (Becton and Dickinson Company, Oxford, UK) through 0.76mm inner diameter capillary tubing (Sterilin, UK). A strong potential difference (…kV) was applied between the needle and a grounded collector using a high voltage supply (FC30 P4 12 W, Glassman Europe Limited, Bramley, UK). The working distance between the EHD gun needle exit and the grounded collector was set to 130 mm. The flow rates of the liquid (…mL/s) were controlled using an ultra-high precision syringe pump (Infuse/Withdraw PHD 4400 Hpsi programmable syringe pump, Harvard Apparatus Ltd, Edenbridge, UK). In order to collect samples, a stationary collector was used.

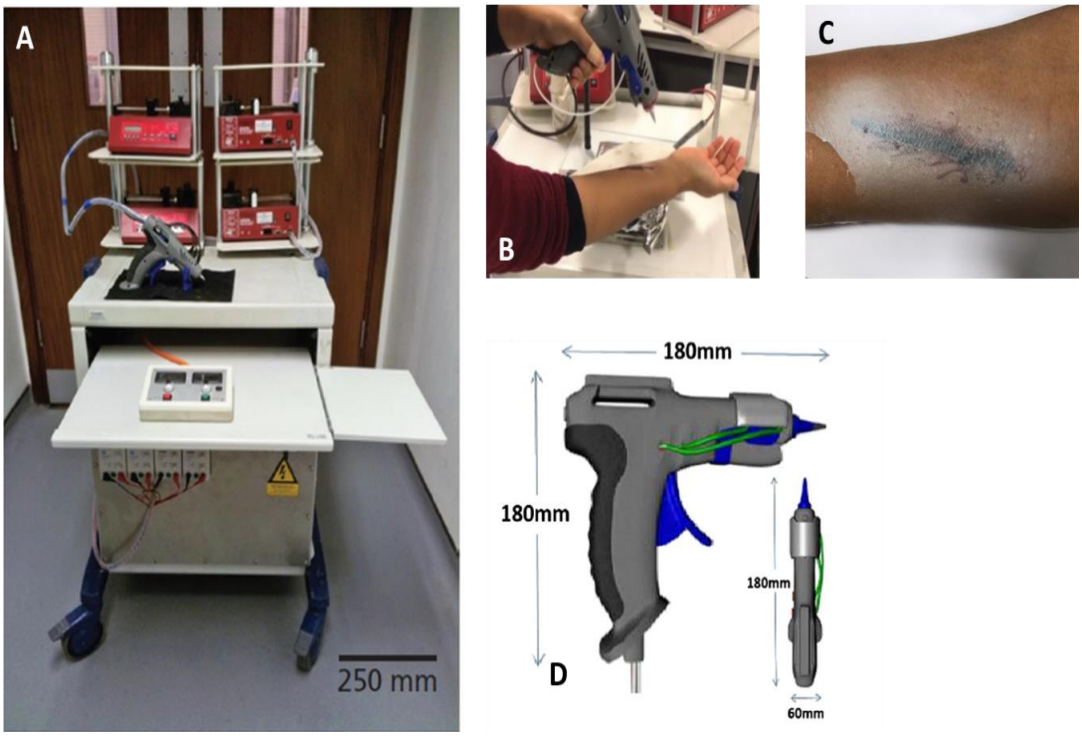


**Fig. 1**. Image of A) portable EHD gun, B) gun in use, C) resulting patch produced *in situ*, and D) a detailed image of the applicator [24]

### *2.4. Crosslinking of nanofibres*

A vacuum desiccator was utilized to dry all nanofibres and thus remove any solvent residue from them. Crosslinking of samples were carried out using GTA vapor. The samples were kept in a sealed glass container and it consists of two parts. The apparatus that divided the glass container has some holes on it and while samples were placed on the upper part, 10 ml of 5 wt% GTA solution was put in a small glass container at the bottom. The whole system was kept in an oven at 40°C for 5 h to create GTA vapor for crosslinking. Then, a vacuum desiccator was utilized for 3 days to remove any residual GTA from the crosslinked samples. During this process, the samples were not moved (kept on waxed paper) and their initial dimensions were preserved in this way. Moreover, the samples were fixed to avoid size reduction during crosslinking [28].

### *2.5. Scanning electron microscopy*

The size and morphology of nanofibres were examined with a scanning electron microscopy (Hitachi VP-SEM S-3400N). The surface of nanofibres was coated with gold for 90 seconds before observation. The average diameter and size distribution of nanofibres were ascertained

by analyzing 100 fibers in randomly recorded SEM micrographs using image software ImageJ (Brocken Symmetry Software).

*2.6. In vitro drug release*

Firstly, encapsulation efficiency was calculated and then drug release tests were performed. In order to calculate encapsulation efficiency, Gel-BC-Gb and Gel-BC-Met were weighed (5 mg) and dissolved in 10 ml of their solvent mixtures in a volumetric flask. The flask was stirred gently over 1 h to provide complete dissolution of Gb and Met from samples into the solvent mixtures. 3 ml of solution was taken and detected using UV-visible spectrophotometer (Jenway 6305, Bibby Scientific, Staffordshire, UK) at 234 nm for Met [29] and 240 nm for Gb [30]. The % encapsulation efficiency was calculated using the equation given below. All measurements were done in triplicate.

$$\text{Encapsulation efficiency} = \frac{\text{mass of actual drug loaded in fibrous scaffolds}}{\text{mass of used in fibrous scaffolds fabrication}} \times 100\%$$

A water bath was used to conduct the drug release tests. Each sample was suspended with gentle shaking in PBS at the ratio of 1 mg of fibrous material to 3 ml of PBS. The sample and PBS were incubated at 37°C for the duration of the test, with a minimum of three test pieces per sample. Each test lasted 15 days with 1 ml of eluent collected every 24 hours and replaced with 1ml of fresh PBS.

*2.7. UV spectroscopy*

A UV spectrophotometer was used to determine the release profiles of metformin and glybenclamide. A calibration curve was constructed for both using standard solutions of known concentrations of each drug. Hence, the amount of drug released from the fibrous patches was determined.

*2.8. Cell viability assay*

L929 (mouse fibroblast) cells were cultured in Dulbecco's Modified Eagle Medium (DMEM) supplemented with 10% fetal bovine serum (FBS) then seeded in 48-well plates at a density of $2.5 \times 10^4$ cells/well and cultured overnight at 37°C and 5% $CO_2$. Cells were treated with each sample for 48 h. After 48 hours incubation, culture medium was replaced with fresh medium and 20 µl MTT solution was added in each well and the plate incubated at 37°C and 5% $CO_2$ for 4 h. After 4 hours, formazan crystals were solubilized by adding 200 µl solubilization buffer

and spectrophotometrical absorbance measured at 550 and 690 nm. The confluent cells were utilized in cytotoxicity tests and SEM investigations.

*2.9. In vivo wound healing experiments*

All animal experiments were carried out with the approval of the Marmara University, Animal Experiments Local Ethics Committee (permission number: 34.2019.mar). Adult male and female Sprague-Dawley rats (250-350 g) (n=12 in each experiment) were obtained from Marmara University Experimental Animal Implementation and Research Center (DEHAMER). The rats were housed under in regulated rooms with controlled temperature (20-23°C), in humidity (40-60%) and light (12 h light/dark regime). The animals were kept on a standard rodent pellet diet, with tap water available ad libitum. All necessary precautions were taken before the experiments and the factors that would negatively affect the parameters were minimized during the study.

*2.9.1. Experimental design of animal test*

Type-1 DM was induced in rats by a single intraperitoneal injection in 60 mg/kg body weight of streptozotocin (STZ), which was prepared in sodium citrate buffer (0.1 mol/L, pH 4.5) immediately before using, following overnight fasting. The diabetic status was confirmed 72 h after STZ injections by measuring blood glucose level collected from tail vein with blood glucose strips (Contour$^{TM}$ PLUS, Bayer Diagnostics). Rats with blood glucose levels greater than 300 mg/dl were considered diabetic and included in the experiment. 10 days after the STZ administration, wound formation studies were performed. In order to begin the experiments, rats were waited on for 10 days to obtain a chronic hyperglycemic state.

After anesthetic administration with intraperitoneal injection of 10 mg/kg xylazine hydrochloride (Rompun) and 25 mg/kg ketamine hydrochloride (Ketalar), the dorsal hair of diabetic rats was completely shaved and the skin was disinfected with povidone-iodine. A sterile biopsy skin punch with a diameter of 8.0 mm (Kai Medical, BP-80F Japan) was placed on both side of the middle back of each rat and a full-thickness wound to the deep facia according to the template was created. The rats were divided into 4 groups, each of 12 rats: control group (no treatment), GEL-BC group (treated with virgin fibre), GEL-BC-Gb group (treated with Gb-loaded fibre), GEL-BC-Met group (treated with Met-loaded fibre). In order to determine the therapeutic effects of each sample on diabetic wound healing, the wounds were completely covered with nanofibrous mats. After covering, the wounds were wrapped with 3M Tegaderm elastic bands (2.2 cm x 2.2 cm, Tegaderm$^{TM}$, 3M Health Care, Germany)

for a day. A self-adhering cover (Nexcare™, 3M Health Care) was used for several hours to ensure that the nanofibrous scaffolds remained on the wounds. No dressing was replaced and no other topical drug was applied during the healing process. Rats were kept in pairs after surgical incisions. Wound margins were* star?? observed and photographed on different days ($0^{th}$, $3^{rd}$, $7^{th}$, $10^{th}$, and $14^{th}$ day after surgical incision) in order to monitor the alteration in the size of the wounds. The area identified by the trace obtained immediately after wounding was used as the original area (day 0 area). Wound closure was expressed as percentage closure of the original wound and was calculated according to following equation:

Wound closure (%) =

(initial wound area – indicated wound area) / initial wound area x 100%

In all groups, the body weight of rats was strictly monitored. The blood of rats was obtained from a tail vein and its glucose content was measured using blood glucose strips. Insulin glargine therapy was administered if the rat lost weight and/or had high glucose level (Sanofi-Aventis, Frankfurt, Germany).

At days 3, 7, and 14, the animals were sacrificed and the entire wound area was collected for further studies. For histopathology, the tissues were embedded in %10 formalin solutions. Additionally, on $14^{th}$ day, the removed wounded area was stored at -80°C for biochemical studies.

*2.10. Histopathological analysis*

For histological examination, wounds together with the surrounding skins were collected at the end of 3rd, 7th and 14th day from all of groups after decapitation and fixed in 10% neutral-buffered formalin for at least 48 h. After fixation, tissue samples were dehydrated in graded ethanol series (%70, 90, 96 and 100), cleared in toluene and embedded in paraffin. Histology analysis was performed from the wound sections (5 µm thick) stained with hematoxylin and eosin (H&E). Each visual field was scored according to re-epithelialization/granulation tissue formation, neutrophil infiltration and edema (Table 1) [31] and measured the wound length using image J programme [32] from at least five animals for each individual treatment.

**Table 1.** Histological scoring of the wound tissue healing

| Score | Epidermal and dermal | Fibroblast density | Neutrophil | Edema |
|---|---|---|---|---|

| | | | | |
|---|---|---|---|---|
| | regeneration | | infiltration | |
| 1 | Little epidermal and dermal organization | Mild fibroblast density | Mild | Mild |
| 2 | Moderate epidermal and dermal organization | Moderate fibroblast density | Moderate | Moderate |
| 3 | Complete remodelling of epidermis and dermis | Increased fibroblast density | Severe | Severe |

*2.11. Biochemical analysis*

Wounded tissue samples were collected after decapitation. Rat wounds were homogenized and supernatant of the homogenates was analyzed using ELISA kits provided from Bioassay Technology Laboratory, Korain Biotech Co., Ltd. (Shanghai, China). All procedures were applied according to the manufacturer's instructions.

*2.12. Statistical analysis*

The interactions between different groups in animal test, histopathological and biochemical analysis were tested using analysis of variance (ANOVA) with 95% confidence interval and Tukey post hoc test. The results were expressed as mean ± standard error mean, and values of $p > 0.05$ were not considered significantly different, whereas values of $p < 0.05$ were considered significant. Data analysis was performed using Graph Pad Prism 6.5 software (Graph Pad, San Diego, CA, USA).

## 3. Results and discussion

*3.1. Production of fibres*

Three batches of fibres were produced Gel-BC-Gb, Gel-BC-Met and Gel-BC, the processing parameters used are listed in Table 2.

**Table 2.** Electrospinning parameters

| Solution | Voltage (kV) | Flow rate (μL $min^{-1}$) | Collector distance (cm) |
|---|---|---|---|
| Gel-BC | 23.5 | 20 | 13 |

| | | | |
|---|---|---|---|
| Gel-BC-Met | 18.0 | 10 | 13 |
| Gel-BC-Gb | 19.7 | 10 | 13 |

*3.2. Morphological and elemental characterisation of fibres*

The Gel-BC-Met, Fig. 2, has a smooth surface with no metformin crystals present on the surface. Metformin is not soluble in acetic acid but it is a suitable solution to dissolve gelatin. However, the gelatin-BC solutions contains DMF as a result of the BC stock solution being made with DMF only. This DMF solubilises the metformin, causing the smooth morphology. The average fibre diameter is 0.22 µm. The Gel-BC-Gb fibres have a larger fibre size, 0.39 µm. This can be attributed to the lower electrical conductivity of the glybenclamide drug, a lower solution conductivity will result in less stretching of the polymer chains as it passes though the electric field, resulting in larger fibre diameters compared to the fibres loaded with metformin.

For Gel-BC-Met, both gelatin and the metformin drug contain nitrogen in their chemical formulae. But, the salt of metformin was used, specifically metformin-HCl ($C_4H_{12}ClN_5$), therefore the chlorine element can be used as an identifier, which is present in both elemental spectra, Fig. 3 and 4.

Glybenclamide contains sulphur and chlorine, which are not present in either of the polymers used in the structure. The elemental spectra of Gel-BC-Gb shows the presence of Cl and S in the polymer construct, which bar contamination, originates from the drug (Fig. 5, 6, 7).

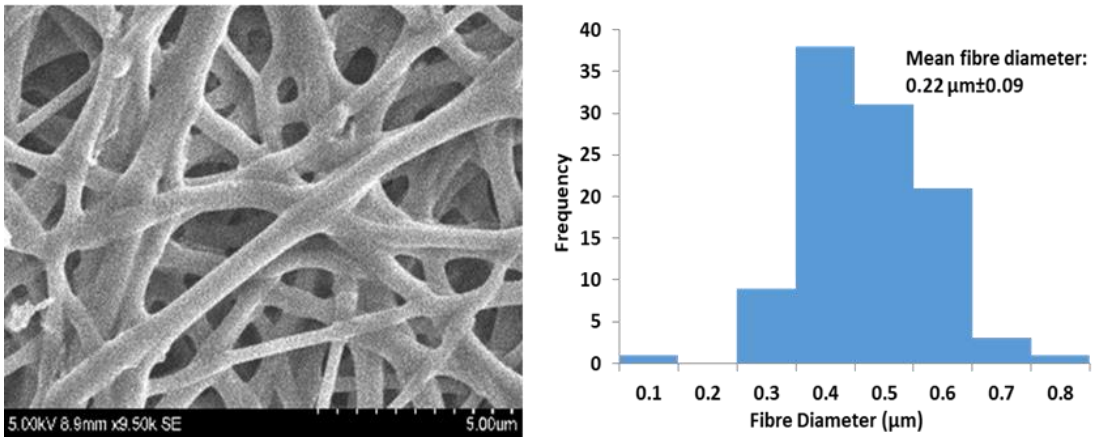


**Fig. 2.** GEL-BC-Met fibres with fibre diameter distribution.

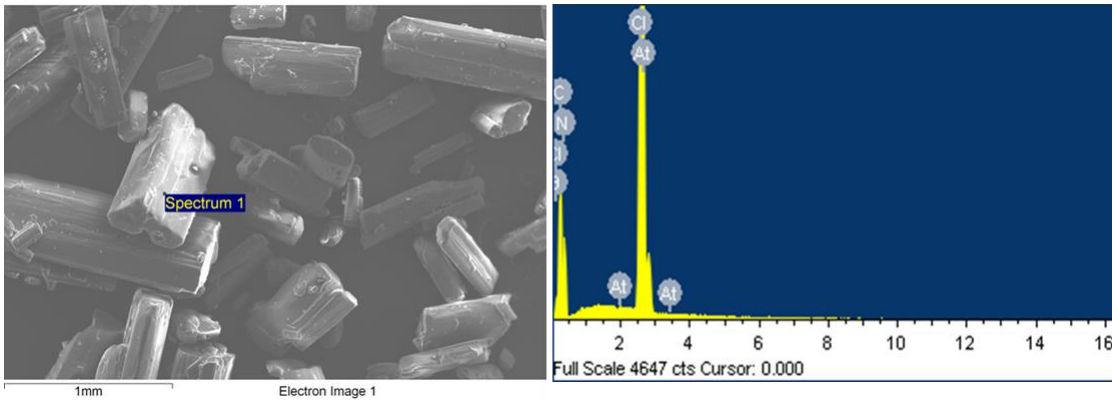


**Fig. 3**. SEM image and elemental dispersive spectrum of Met.

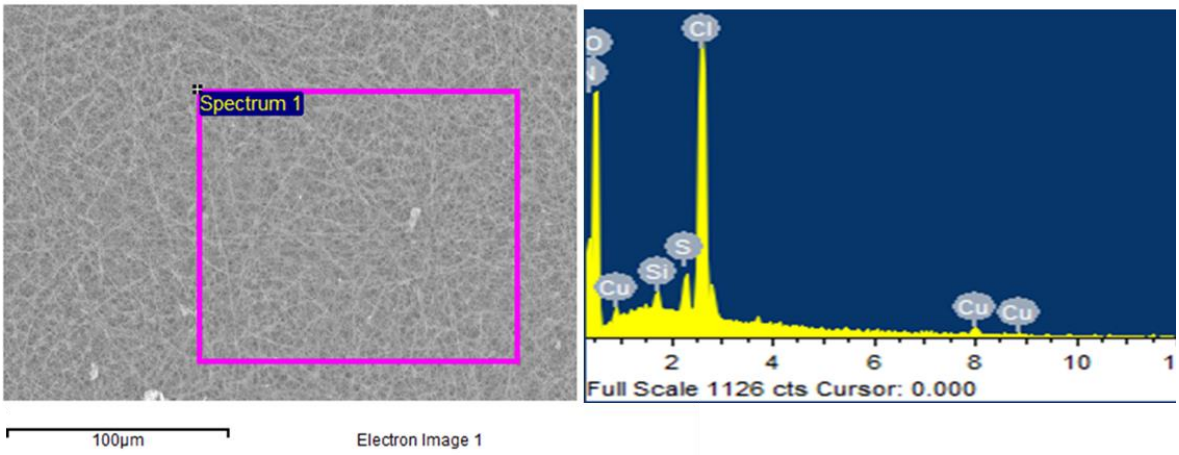


**Fig. 4.** SEM image and elemental dispersive spectrum of Gel-BC-Met.

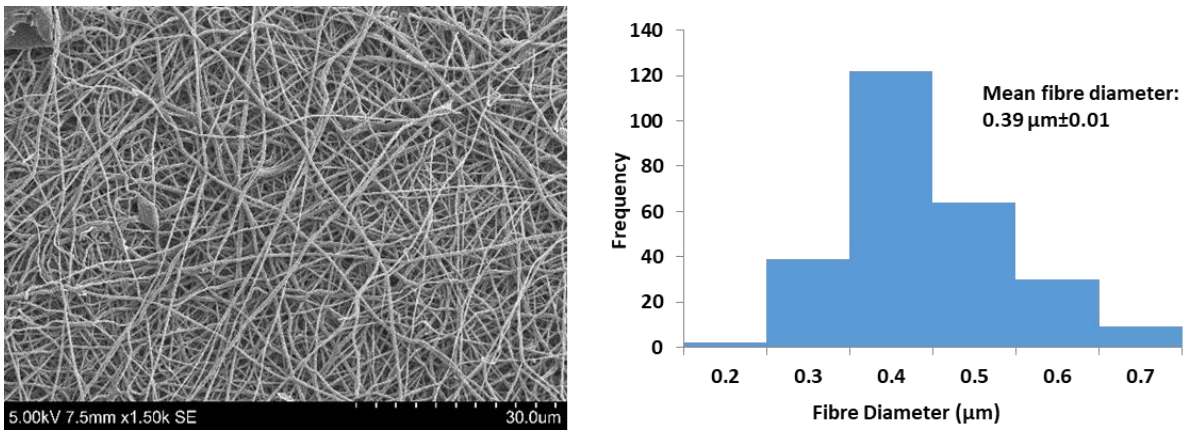


**Fig. 5**. GEL-BC-Gb fibres with fibre diameter distribution.

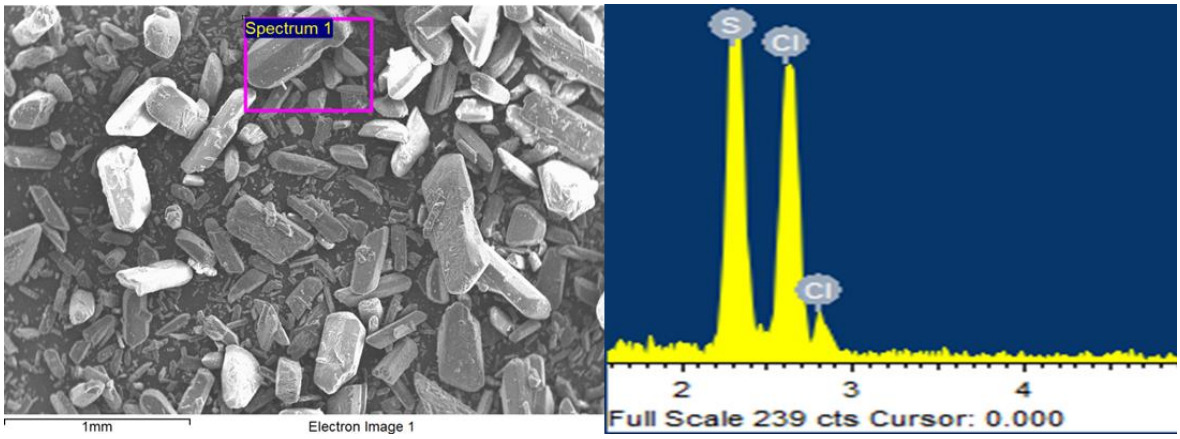


**Fig. 6**. SEM image and elemental dispersive spectrum of Gb.

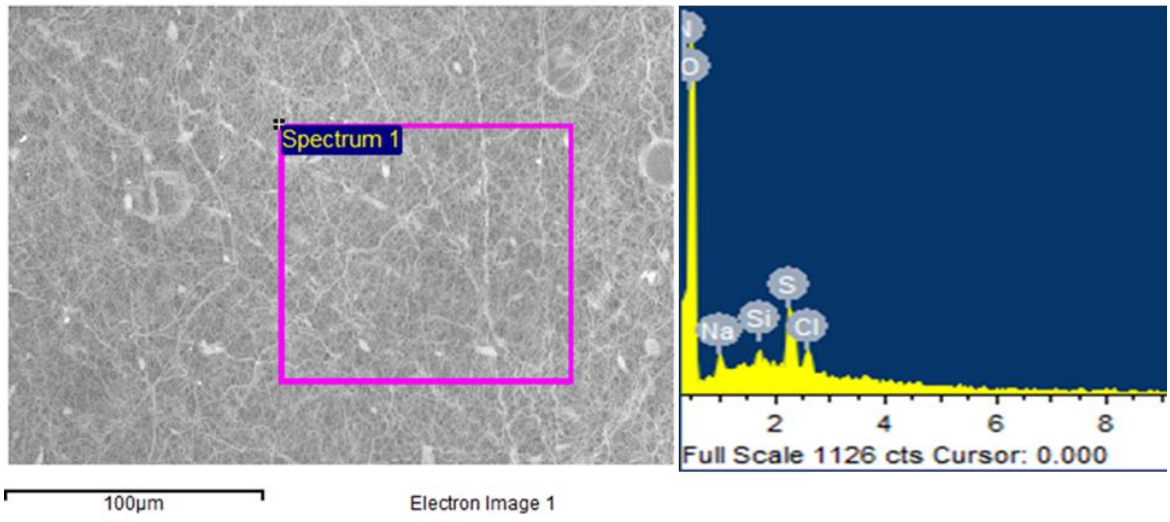


**Fig. 7**. SEM image and elemental dispersive spectrum of Gel-BC-Gb.

*3.3. In vitro drug release profiles*

The encapsulation efficiencies within the samples were calculated and it was ~78% for Gel-BC-Gb and ~80% for Gel-BC-Met. Crosslinking is necessary to ensure the fibres do not lose their structure, especially for this intended application of highly exudating diabetic wounds. This will have a knock on effect on the release behaviour of the polymer construct, essentially reducing the drug released. However, the hydrophilic nature of BC draws PBS into the fibre which may speed up the hydrolysis of gelatin counteracting the effect of the crosslinking in both Gel-BC-Met and Gel-BC-Gb [33]. Metformin released follows a near linear profile (Figure 8), demonstrating a sustained release, peaking on day 15 at approximately 0.0197 mg. The release of Gb from the Gel-BC matrix is not as smooth and may be indicative of some interaction between the polymer, either gelatin or BC. There is a segment of burst release, may

be due to breakdown of fibre or crosslinking, shown between day 4 and 6 in Fig 9. The profile peaks at day 10 with 0.024 mg.

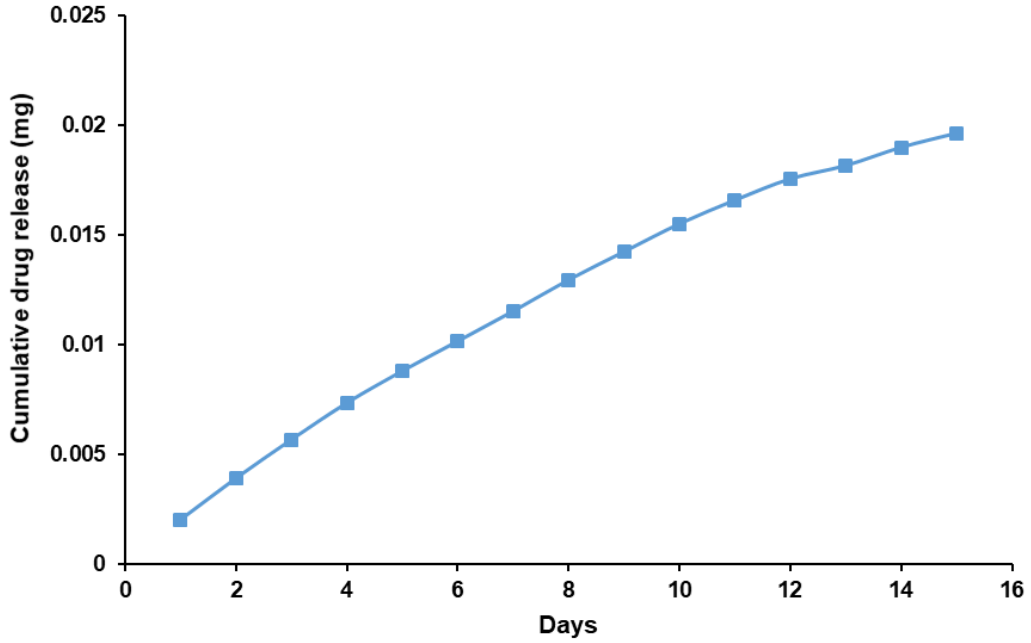


**Fig. 5**. Release of Met from Gel-BC-Met fibres according to first-order model. All the values were obtained from the averages of three experiments, and the errors were less than 5%.

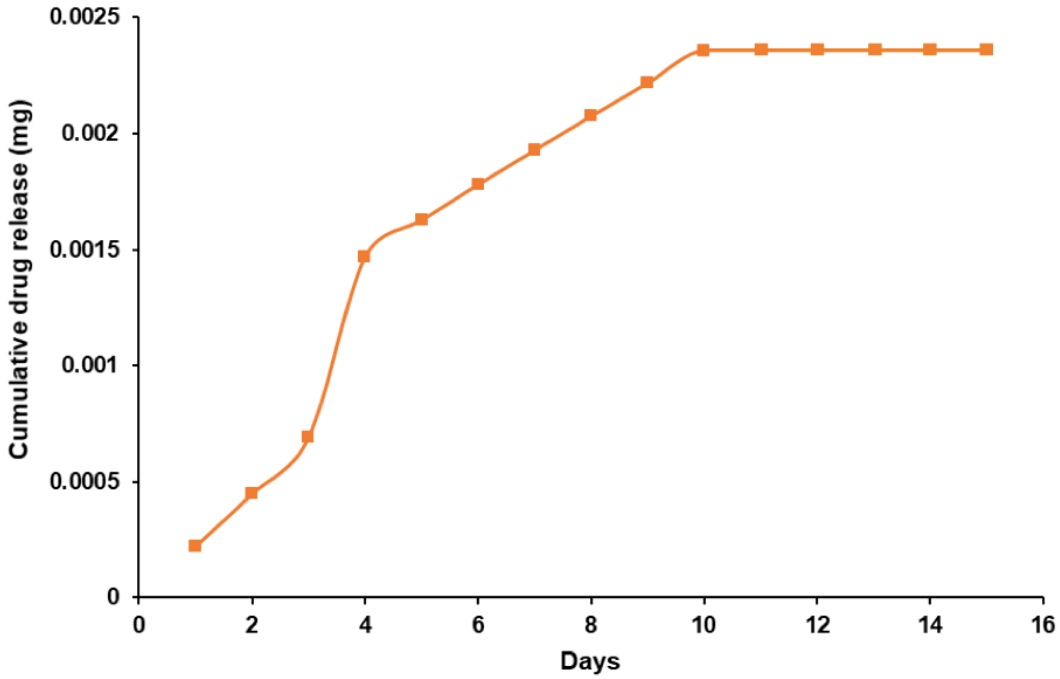


**Fig. 6**. Release of Gb from Gel-BC-Gb fibres according to first-order model. All the values were obtained from the averages of three experiments, and the errors were less than 5%.

*3.4. Cell viability*

Fig. 10 shows the cytotoxicity of the fibres on L929 mouse fibroblast cells in 48h using MTT assay. The results demonstrated that the virgin fibre group exhibited a significant effect on the proliferation of fibroblast cells, on the contrary by adding 20% DMSO (STATE 20% WT OR VOL ) decreased the cell viability less than 10%. When drugs were added into fibre, the fibroblast proliferation decreased as seen in GEL-BC-Gb and GEL-BC-Met groups. However, there is no significant difference between drug-loaded fibres and control group. Also, the cell viability of negative control group and drugs-loaded fibre groups demonstrated similar results. There is a significant difference between all fibre groups and 20% DMSO. Therefore, it is clearly seen that all fibre samples can safely be applied on the wound site without risk of cytotoxicity.

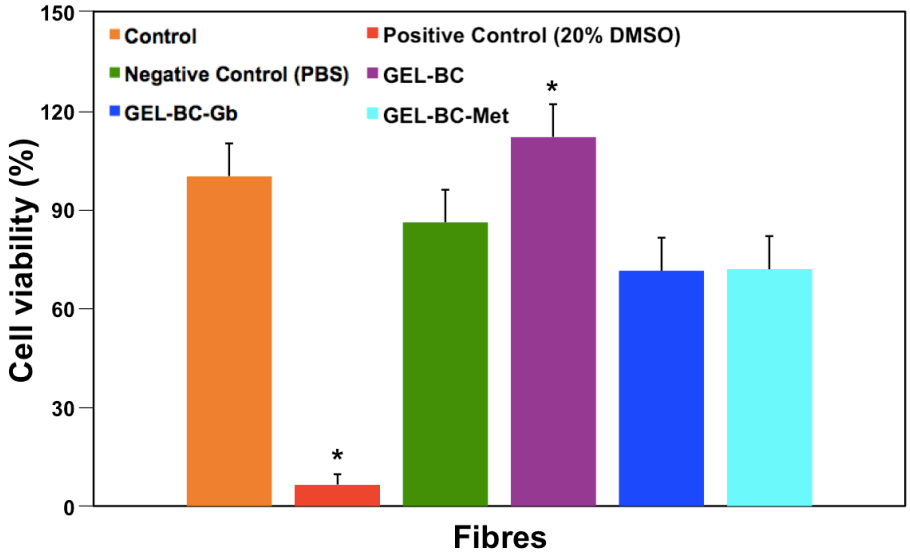


**Fig. 10.** L929 (mouse fibroblast) cell viability of Gel-BC, GEL-BC-Gb, and GEL-BC-Met fibres. The data were presented as mean ± standard error of the mean. *$p < 0.05$ versus control group. The statistical analyses were carried out with ANOVA test and the Tukey post hoc test.

*3.5. In vivo wound healing effect*

Wound closure was monitored in type-1 diabetic rats and Fig. 11a shows the wound closure images of wounds treated with various fibres taken on days 0, 3, 7, 10, and 14. Wound closure in type-1 diabetic rats was measured from day 0 to day 14 as percentage in Fig. 11b. There is no significant difference in wound closure between control and GEL-BC groups on day 3. Around 20% wound closure was observed in these groups. However, drug-loaded fibres significantly decreased the wound area compared to control group (~25%, $p < 0.01$). On day 7,

GEL-BC-Gb and GEL-BC-Met group decreased to 37.1 ± 4.3% and 46.6 ± 1.3% , respectively. Moreover, GEL-BC-Gb group showed a better recovery ($p < 0.01$) than GEL-BC-Met group. Similar results were observed on Day 10 and Gb-loaded fibre was better than Met-loaded fibre (decreased to 13.2 ± 2.4% vs. 20.4 ± 0.8%) . Different from previous days, for the first time, the virgin fibre group (GEL-BC) was significanlty better than control group on day 10. At the last day of the experiment, drug-loaded fibre groups showed better recovery than the other groups ($p < 0.01$). Gb and Met significantly accelarated diabetic wound healing.

Wound healing is a process divided into four phases: (i) hemostasis, (ii) inflammation, (iii) proliferation, and (iv) remodelling. In details, the inflammatory phase lasts around 6 days following injury and several leucocytes like macrophages migrates into the wound area. The proliferative phase involves proliferation of fibroblast and keratinocytes and occurs between days 4 and 10 following wound creation. Remodeling phase begins around day 7 and formation of extracellular matrix and collagen fibers rise during this phase. The healing process is not well orchestrated due to excessive inflammatory reactions in diabetes [6, 34, 35]. In this study, the wound healing effect of Gb and Met began from day 3 and lasted to day 14.

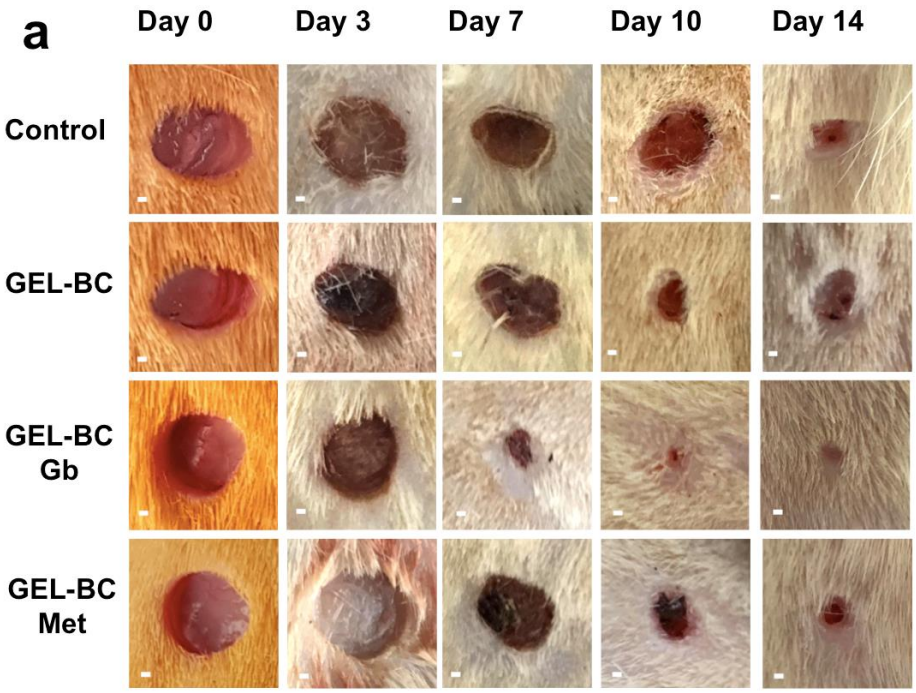

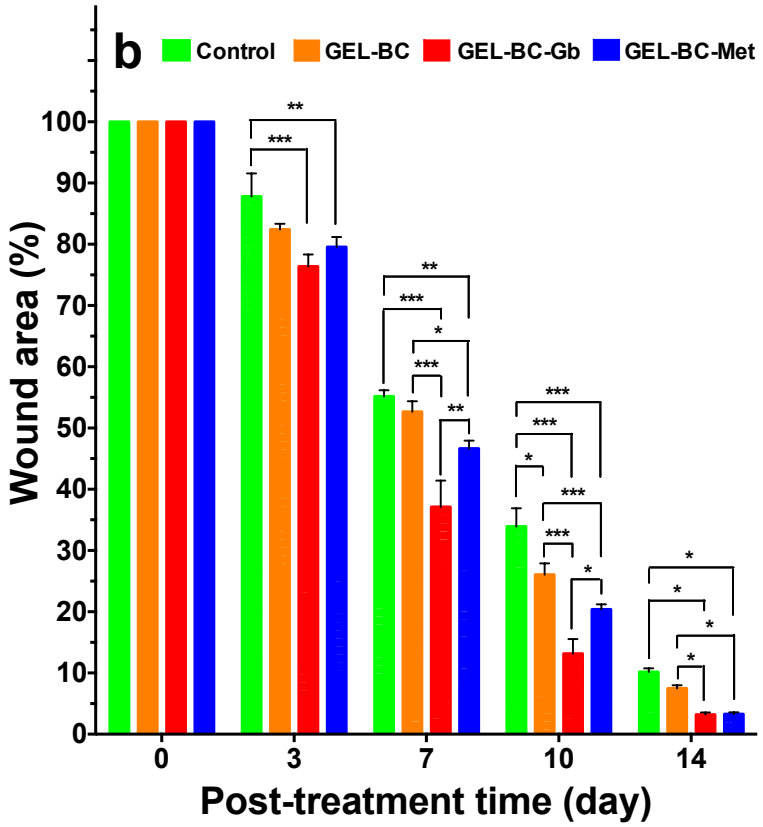


**Fig. 11.** *In vivo* wound healing in diabetic rats. (a) Appearance of healing wound on days 0, 3, 7, 10, and 14 after surgical incision (scale bar = 1 cm). (b) Change in wound area after various treatments. The data was presented as mean ± standard error of the mean. Values are represented statistically when *p < 0.05, **p < 0.01, ***p < 0.001 in comparison with each other. The statistical analyses were carried out with ANOVA test and the Tukey post hoc test.

*3.6. Histological analysis*

Results of gross appearances are shown in Fig. 12a and wound length measurements are given in Fig. 12b. The determination of the histological findings is shown in Fig. 12c throughout the experiments according to the criteria in Table 1.

In all groups on day 3, severe epidermis/dermis degeneration, neutrophil infiltration along with increased bleeding and edema were observed. However, no fibroblasts were observed. Histological examination of wounds of the control and virgin fibre group (GEL-BC) at day 7 showed incomplete re-epithelialization, crusting, and poorly-formed and immature granulation tissue formation. A prominent infiltration of inflammatory cells mainly composed of neutrophils within the wound margins and in the deep dermis was observed. Tissue edema and haemorrhage were evident. In GEL-BC-Met and GEL-BC-Gb groups, re-epithelialization was

moderate, still persisting both focal spongiosis and scab. Granulation tissue appeared partially organized with slight edema.

Diabetic wounds treated with GEL-BC-Met at day 14 were characterized by moderate re-epithelialization, and partially organized granulation tissue. Moderate to complete re-epithelialization and well-formed granulation tissue were observed in diabetic wounds treated with GEL-BC-Gb at day 14. The histologic scores obtained at day 14 confirmed that GEL-BC-Gb group played a stronger wound-healing role compared to GEL-BC-Met group. In addition, GEL-BC-Gb and GEL-BC-Met applied into the wounds of diabetic animals improved wound closure compared to control and GEL-BC groups. Drug-loaded fibre groups significantly decreased wound length on day 7 and 14 compared to control and GEL-BC groups. GEL-BC-Gb group significantly decreased ($p<0.05$) wound length more than GEL-BC-Met group in both day 7 and 14.

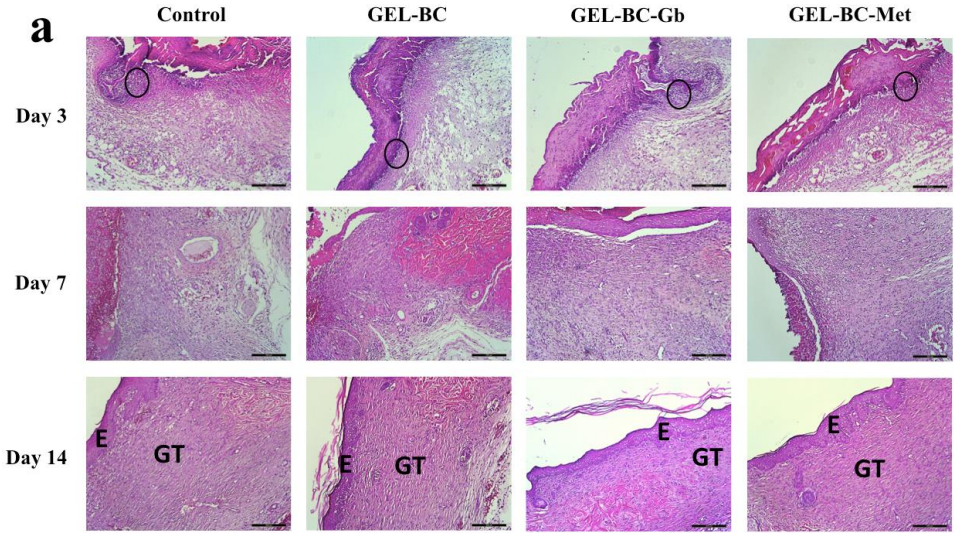

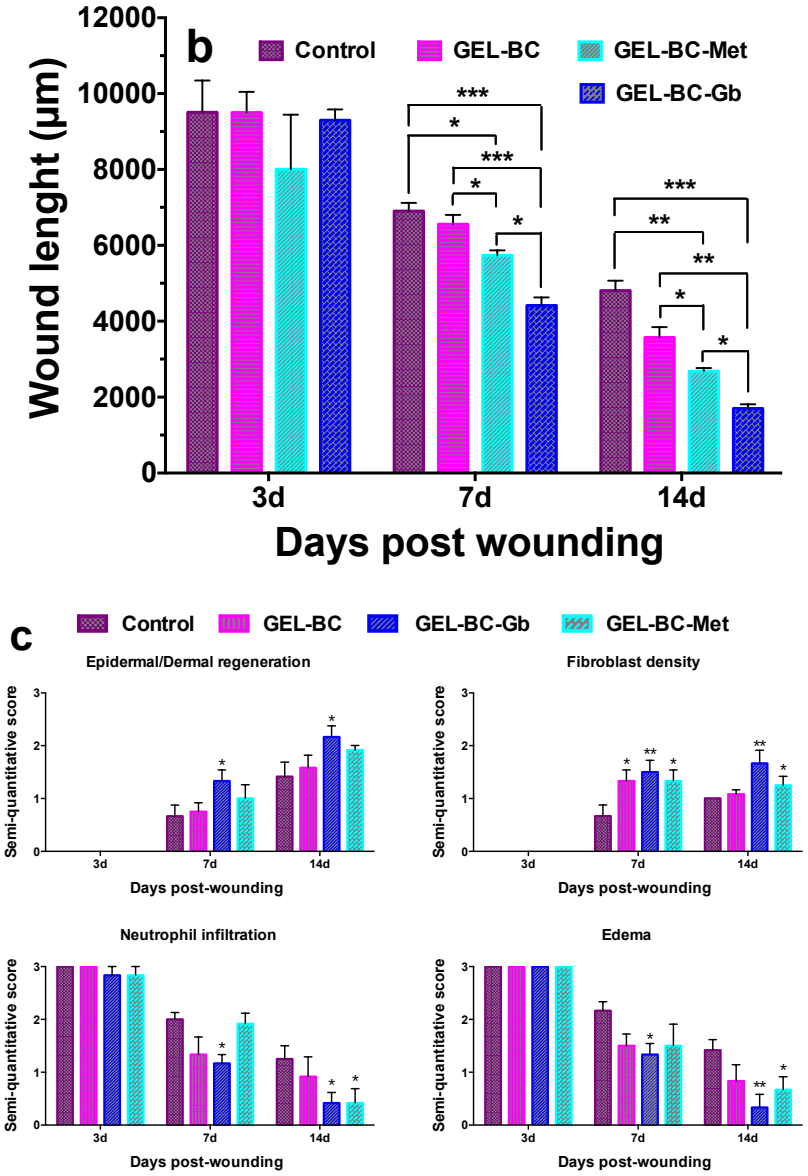


**Fig. 12.** Histopathological evaluations. (a) Representative microscopic images of wounds from control, GEL-BC, GEL-BC-Gb, and GEL-BC-Met groups at day 3, 7 and 14. The circles indicate neutrophil infiltration. GT: granulation tissue. E: epithelium. Hematoxylin and eosin staining. Scale bars: 200 µm. (b) Comparison of wound length for all groups at day 3, 7, and 14. (c) Histological scoring on days 3, 7, and 14. The values were calculated as the mean ± standard error mean (n=6), ***p< 0.001, **p< 0.01, *p< 0.05. The statistical analyses were carried out with ANOVA test with the Tukey post hoc test.

*3.7. Biochemical analysis*

TNF-α level was measured according to the manufacturer instruction using ELISA kit in the wound areas on day 14 (Fig. 13). Expression level of TNF-α was significantly lower in all

treatment ($p<0.001$) and GEL-BC ($p<0.05$) groups compared to control group. Also, the level of TNF-α in the treatment groups was significantly lower ($p<0.01$) than those in GEL-BC group. The highest decrease of TNF-α level was observed in GEL-BC-Gb group at the end of the experiment but there is no significant difference between drug-loaded fibre groups.

TNF-α is one of the primary pro-inflammatory cytokines involved in the migration of immune cells and plays a key role in the inflammatory phase. It is known in the literature that the level of TNF-α is higher in chronic wounds. It was observed that TNF-α level was significantly lower in biochemical analysis at the end of day 14 in accordance with the histological findings in drug-loaded fibre treated groups.

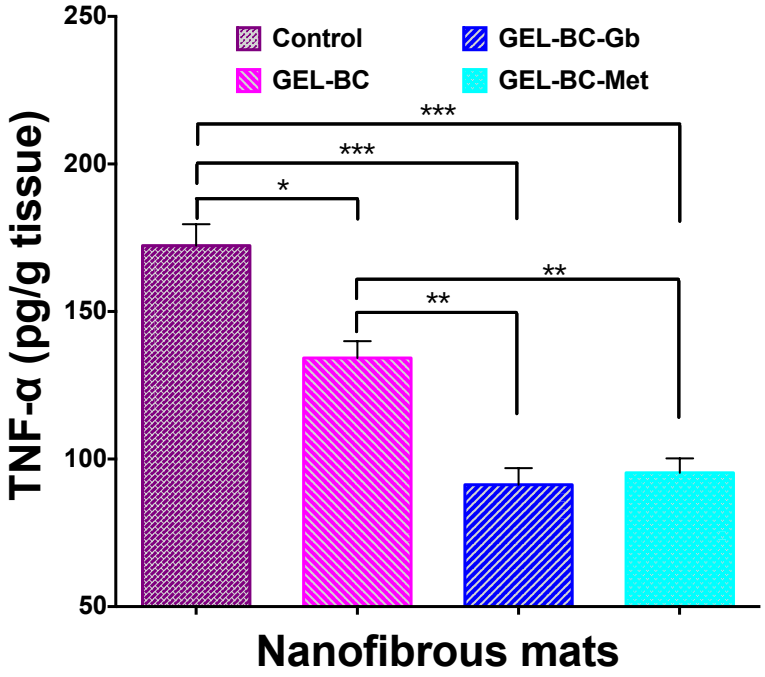


**Fig. 13.** The level of tumor necrosis factor-alpha (TNF-α) in the wounded area of all groups on day 14 after surgical incision. The statistical analyses were carried out with ANOVA test and the Tukey post hoc test. Values are represented statistically when *$p < 0.05$, **$p < 0.01$, ***$p < 0.001$.

## 4. Conclusions

Met and Gb were successfully loaded into GEL/BC fibre using a portable, point of need electrospinning set up. Morphological evaluation, physical and chemical composition, thermal properties, drug release behaviors, and in-vitro cytotoxicity evaluation of all fibres were

investigated. Also, their effects on diabetic wound healing were histologically and biochemically compared in vivo. GEL-BC-Gb group showed a better recovery than GEL-BC-Met group in the animal test without risk of cytotoxicity. The histologic scores obtained at day 14 confirmed that GEL-BC-Gb group played a stronger wound-healing role compared to GEL-BC-Met group. The highest decrease of TNF-α level was observed in GEL-BC-Gb group at the end of the experiment but there is no significant difference between drug-loaded fibre groups. Met and Gb-loaded fibres in a sustained release form has high potential for diabetic wound healing with high bioavailability and fewer systemic side effects.

**Acknowlegments**

The authors are grateful to the UK Engineering & Physical Sciences Research Council (EPSRC) for funding pressurized gyration forming research at University College London (Grants EP/S016872/1 and EP/N034228/1). All data pertaining to this research is in the manuscript. Dr. Muhammet E. Cam was supported by a TUBITAK 2219 Research Programme Grant (Scientific and Technological Research Council of Turkey-TUBITAK) and thanks UCL Mechanical Engineering for hosting his post-doctoral research in the UK.

**References**

[1] M.E. Cam, A.N. Hazar-Yavuz, S. Yildiz, B. Ertas, B. Ayaz Adakul, T. Taskin, S. Alan, L. Kabasakal, The methanolic extract of Thymus praecox subsp. skorpilii var. skorpilii restores glucose homeostasis, ameliorates insulin resistance and improves pancreatic β-cell function on streptozotocin/nicotinamide-induced type 2 diabetic rats, J. Ethnopharmacol. 231 (2019) 29-38.

[2] M.E. Cam, S. Yildiz, B. Ertas, A.E. Acar, T. Taskin, L. Kabasakal, Antidiabetic effects of Salvia triloba and Thymus praecox subsp. skorpilii var. skorpilii in a rat model of streptozotocin/nicotinamide-induced diabetes. Marmara Pharm. J. 21 (201), 818-827.

[3] A. American Diabetes, Diagnosis and classification of diabetes mellitus, Diabetes Care 32 Suppl 1(Suppl 1) (2009) S62-S67.

[4] R.E. Mirza, M.M. Fang, W.J. Ennis, T.J. Koh, Blocking Interleukin-1β Induces a Healing-Associated Wound Macrophage Phenotype and Improves Healing in Type 2 Diabetes, Diabetes 62(7) (2013) 2579.

[5] R. Mirza, T.J. Koh, Dysregulation of monocyte/macrophage phenotype in wounds of diabetic mice, Cytokine 56(2) (2011) 256-264.

[6] M.E. Cam, S. Yildiz, H. Alenezi, S. Cesur, G.S. Ozcan, G. Erdemir, U. Edirisinghe, D. Akakin, D.S. Kuruca, L. Kabasakal, O. Gunduz, M. Edirisinghe, Evaluation of burst release and sustained release of pioglitazone-loaded fibrous mats on diabetic wound healing: an in vitro and in vivo comparison study, J. R. Soc. Interface 17(162) (2020) 20190712.

[7] R.E. Mirza, M.M. Fang, E.M. Weinheimer-Haus, W.J. Ennis, T.J. Koh, Sustained Inflammasome Activity in Macrophages Impairs Wound Healing in Type 2 Diabetic Humans and Mice, Diabetes 63 (2014) 1103-1114.

[8] K. Koshiba, M. Nomura, Y. Nakaya, S. Ito, Efficacy of glimepiride on insulin resistance, adipocytokines, and atherosclerosis, J. Med. Investig. 53(1,2) (2006) 87-94.

[9] M. Lamkanfi, J.L. Mueller, A.C. Vitari, S. Misaghi, A. Fedorova, K. Deshayes, W.P. Lee, H.M. Hoffman, V.M. Dixit, Glyburide inhibits the Cryopyrin/Nalp3 inflammasome, J. Cell. Biol. 187 (2009) 61-70.

[10] N. Nath, M. Khan, M.K. Paintlia, M.N. Hoda, S. Giri, Metformin Attenuated the Autoimmune Disease of the Central Nervous System in Animal Models of Multiple Sclerosis, J. ımmunol. 182 (2009) 8005-8014.

[11] C.H. Lee, M.J. Hsieh, S.H. Chang, Y.H. Lin, S.J. Liu, T.Y. Lin, K.C. Hung, J.H. Pang, J.H. Juang, Enhancement of diabetic wound repair using biodegradable nanofibrous metformin-eluting membranes: in vitro and in vivo, ACS Appl. Mater. Interfaces 6(6) (2014) 3979-86.

[12] M. Arai, M. Uchiba, H. Komura, Y. Mizuochi, N. Harada, K. Okajima, Metformin, an Antidiabetic Agent, Suppresses the Production of Tumor Necrosis Factor and Tissue Factor by Inhibiting Early Growth Response Factor-1 Expression in Human Monocytes in Vitro, J. Pharmacol. Exp. Ther. 334 (2010) 206-213.

[13] J. Ahmed, M. Gultekinoglu, M. Edirisinghe, Bacterial cellulose micro-nano fibres for wound healing applications, Biotechnol. Adv. (2020) 107549.

[14] J.D. Fontana, de Sousa, A. M., Fontana C. K., Torriani I. L., Moreschi, J. C., Galloti, B. J., de Sousa, S. J., Narcisco, G. P., Bichara, J. A., Farah, L. F., Acetobacter cellulose pellicles as a temporary skin substitute, Appl. Biochem Biotechnol. 24(25) (1990) 253-264.

[15] W. Czaja, Krystynowicz, A., Bielecki, S., Brown, R. M., Microbial cellulose-the natural power to heal wounds, Biomaterials 27(2) (2006) 145-151.

[16] V.I. Legeza, Galenko-Yaroshevskii, V. P., Zinov'ev, E. V., Paramonov, B. A., Kreichman, G. S., Karnovich, A. G., Khripunov, A. K., Effects of new wound dressings on healing of thermal burns of the skin in acute radiation disease, B. Exp. Biol. Med. 138(3) (2004) 311-315.

[17] G. Gayathry, Gopalawasmy, G., Production and characterisation of microbial cellulosic fibre from Acetobacter xylinum, Indian J. Fibre Text. 39 (2012) 93-96.

[18] H.M. Powell, S.T. Boyce, Fiber density of electrospun gelatin scaffolds regulates morphogenesis of dermal–epidermal skin substitutes, J. Biomed. Mater. Res. A 84A(4) (2008) 1078-1086.

[19] H. Alenezi, M.E. Cam, M. Edirisinghe, Experimental and theoretical investigation of the fluid behavior during polymeric fiber formation with and without pressure, Appl. Phys. Rev. 6(4) (2019) 041401.

[20] Y.-S. Lim, Y.-J. Ok, S.-Y. Hwang, J.-Y. Kwak, S. Yoon, Marine Collagen as A Promising Biomaterial for Biomedical Applications, Mar. Drugs 17(8) (2019) 467.

[21] Y. Chen, X. Zhou, Q. Lin, D. Jiang, Bacterial cellulose/gelatin composites: In situ preparation and glutaraldehyde treatment, Cellulose 21 (2014).

[22] M.T. Arafat, G. Tronci, D. Wood, S. Russell, In-situ crosslinked wet spun collagen triple helices with nanoscale-regulated ciprofloxacin release capability, Mater. Lett. 255 (2019) 126550.

[23] M. Bazbouz, H. Liang, G. Tronci, A UV-cured nanofibrous membrane of vinylbenzylated gelatin-poly(epsilon-caprolactone) dimethacrylate co-network by scalable free surface electrospinning, Mater. Sci. Eng. C 91 (2018) 541-555.

[24] P. Sofokleous, E. Stride, W. Bonfield, M. Edirisinghe, Design, construction and performance of a portable handheld electrohydrodynamic multi-needle spray gun for biomedical applications, Mat. Sci. Eng. C-Mater. 33(1) (2013) 213-223.

[25] W.K. Lau, P. Sofokleous, R. Day, E. Stride, M. Edirisinghe, A portable device for in situ deposition of bioproducts, Bioinspired Biomim. Nanobiomat. 3(2) (2014) 94-105.

[26] M.O. Aydogdu, E. Altun, M. Crabbe- Mann, F. Brako, F. Koc, G. Ozen, S.E. Kuruca, U. Edirisinghe, C.J. Luo, O. Gunduz, M. Edirisinghe, Cellular interactions with bacterial cellulose: Polycaprolactone nanofibrous scaffolds produced by a portable electrohydrodynamic gun for point- of- need wound dressing, Int. Wound J. 15(5) (2018) 789-797.

[27] P. Sofokleous, E. Stride, M. Edirisinghe, Preparation, characterization, and release of amoxicillin from electrospun fibrous wound dressing patches, Pharm. Res. 30(7) (2013) 1926-38.

[28] S. Gomes, G. Rodrigues, G. Martins, C. Henriques, J.C. Silva, Evaluation of nanofibrous scaffolds obtained from blends of chitosan, gelatin and polycaprolactone for skin tissue engineering, Int. J. Biol. Macromol. 102 (2017) 1174-1185.

[29] Y.D. Dange, S. Honmane, S. Bhinge, V. Rajaram Salunkhe, D. Raghunath Jadge, Development and Validation of UV-Spectrophotometric Method for Estimation of Metformin in Bulk and Tablet Dosage Form, Indian J. Pharm. Educ. 51(4s) (2017) 754-760.

[30] N. Haq, F.K. Alanazi, I.A. Alsarra, F. Shakeel, Rapid Analysis of Glibenclamide Using an Environmentally Benign Stability-Indicating RP-HPLC Method, Iran J. Pharm. Res. 13(3) (2014) 863-872.

[31] A. Bitto, N. Irrera, G. Pizzino, G. Pallio, F. Mannino, M. Vaccaro, V. Arcoraci, F. Aliquò, L. Minutoli, M.R. Colonna, M.R. Galeano, M. Brines, C. De Ponte, M. Collino, F. Squadrito, D. Altavilla, Activation of the EPOR-β common receptor complex by cibinetide ameliorates impaired wound healing in mice with genetic diabetes, Biochimica et Biophysica Acta (BBA) - Mol. Basis Dis. 1864(2) (2018) 632-639.

[32] N.S. Tan, W. Wahli, Studying Wound Repair in the Mouse, Curr. Protoc. Mouse Biol. 3(3) (2013) 171-185.

[33] W. Czaja, A. Krystynowicz, S. Bielecki, R.M. Brown, Jr., Microbial cellulose--the natural power to heal wounds, Biomaterials 27(2) (2006) 145-51.

[34] M. Xue, C.J. Jackson, Extracellular Matrix Reorganization During Wound Healing and Its Impact on Abnormal Scarring, Adv. Wound Care (New Rochelle) 4(3) (2015) 119-136.

[35] A.C.d.O. Gonzalez, T.F. Costa, Z.d.A. Andrade, A.R.A.P. Medrado, Wound healing - A literature review, An. Bras. Dermatol. 91(5) (2016) 614-620.